


Effective Hamiltonians in the quantum Rabi problem

P. Gartner  and V. Moldoveanu *

National Institute of Materials Physics, P.O. Box MG-7, Bucharest-Magurele, Romania

 (Received 2 June 2021; accepted 24 January 2022; published 4 February 2022)

We revisit the theoretical description of the ultrastrong light-matter interaction in terms of exactly solvable effective Hamiltonians. A perturbative approach based on polaronic and spin-dependent squeezing transformations provides an effective Hamiltonian for the quantum Rabi model up to the second order in the expansion parameter. The model consistently includes both rotating and counter-rotating terms, going therefore beyond the rotating-wave approximation. Analytical and numerical results show that the proposed Hamiltonian performs better than the Bloch-Siegert model when calculating operator averages (e.g., the mean photon number and number of excitations). This improvement is due to a refined calculation of the dressed states within the present model. Regarding the frequency shift induced by the qubit-photon interaction, we find a different sign from the Bloch-Siegert value. This influences the structure of the eigenstates in a nontrivial way and ensures the correct calculation of the number of excitations associated with a given dressed state. As a consistency check, we show that the exactly solvable independent boson model is reproduced as a special limit case of the perturbative Hamiltonian.

DOI: [10.1103/PhysRevA.105.023704](https://doi.org/10.1103/PhysRevA.105.023704)

I. INTRODUCTION

The physics of strongly coupled qubit-photon hybrid systems has become a steadily developing field [1,2] which challenges the existing theoretical methods. In particular, as the field-matter coupling strength increases, the Jaynes-Cummings model [3], which neglects the so-called off-resonant transitions within the rotating-wave approximation (RWA), becomes less accurate.

More general models taking fully into account the interaction between a two-level system (e.g., a superconducting qubit or a quantum dot) and a boson mode (cavity photon or transmission line resonator) are defined by the class of Hamiltonians

$$H = \frac{1}{2}\varepsilon\sigma_z + \omega a^\dagger a + g_1(a^\dagger\sigma + a\sigma^\dagger) + g_2(a^\dagger\sigma^\dagger + a\sigma), \quad (1)$$

where the quasispin notation is used for the qubit and a and a^\dagger are bosonic operators of the single-mode field. The corresponding energies are ε and ω , respectively, and g_1 and g_2 are the coupling strengths for the resonant (rotating) and off-resonant (counter-rotating) processes. We take $\hbar = 1$ throughout. The Jaynes-Cummings (JC) Hamiltonian is then recovered from Eq. (1) by taking $g_2 = 0$, while the quantum Rabi model (QRM) [4,5] corresponds to $g_1 = g_2 = g$:

$$H_R = \frac{1}{2}\varepsilon\sigma_z + \omega a^\dagger a + g\sigma_x(a^\dagger + a). \quad (2)$$

Generally, the problems defined by Eq. (1) are not exactly soluble, one notable exception being the quantum Rabi Hamiltonian whose spectrum was calculated [6–8] as zeros of recursively defined new special functions or in terms of con-

fluent Heun functions [9]. The mathematics is quite involved both for the eigenvalues and for the eigenvectors.

In view of this situation, in the literature one prefers to devise effective Hamiltonians [2] to obtain approximate eigenvalues and eigenvectors, in suitably restricted domains of the parameter space defined by $\{\varepsilon, \omega, g\}$. Such effective Hamiltonians capture important effects of the counter-rotating terms in qubit-photon interaction. For instance, the presence of qubit-resonator excitations in the ground state is well described by such simpler approximations [2]. Also, they account for the Bloch-Siegert shifts of qubit and resonator frequencies [10] or the multiphoton Rabi oscillations in superconducting qubits coupled to transmission-line resonators [11].

On the other hand, the 2×2 block-diagonal structure of the effective Hamiltonians and the analytical JC-like eigenfunctions are more suitable for numerical implementation. In contrast, the exact dressed states of the Rabi Hamiltonian (even when calculated by numerical diagonalization in a truncated Fock space) “spread” over many photon Fock states. This feature makes the physical discussion of the allowed transitions more cumbersome and less intuitive.

This is why simple, analytic effective descriptions are strongly preferred when such transitions occur due to additional interactions needed to describe optical [11,12], transport [13,14], or relaxation processes [12,15]. In these cases the implementation of a Lindblad master equation and the calculation of the corresponding dissipative kernels must be performed with respect to the dressed states basis, a task that is greatly simplified in the effective Hamiltonian picture.

A useful test for these approximations consists of inspecting limit cases in which exact solutions are known for the full Hamiltonian. One such case is the JC model mentioned

*Corresponding author: valim@infim.ro

above, in which the RWA brings the Hamiltonian to a 2×2 block-diagonal form. A second one is the independent boson model (IBM) [16] which is extensively used for quantum optical and transport calculations involving carrier interaction with photons, phonons [17], or vibrons [18]. In the present case the IBM limit is obtained by taking $\varepsilon = 0$ in the QRM, Eq. (2), and the corresponding Hamiltonian is diagonalized by a displacement of the bosonic oscillator centers brought in by the Lang-Firsov or polaronic unitary transform.

In deriving approximate effective Hamiltonians for the quantum Rabi problem one usually employs a limited expansion of various unitary transforms in terms of a suitable small parameter. An example is provided by the dispersive Hamiltonian [19,20] obtained by a unitary transform aiming at diagonalizing the qubit-boson interaction, expanded to second order in the parameter $\lambda = g/|\varepsilon - \omega|$, in the weak-coupling limit $\lambda \ll 1$. The resulting effective Hamiltonian reproduces the JC spectrum to second order in λ , i.e., within the domain of parameters in which it was derived. Moreover, it recovers the exact result in the IBM limit.

Another popular effective Hamiltonian is the Bloch-Siegert (BS) one [21,22]. It treats the QRM problem up to second order in the parameter $\lambda = g/(\varepsilon + \omega)$ and brings it to a renormalized form of the JC Hamiltonian. Two successive unitary transforms are used in the process and higher-order off-resonant terms are discarded as rapidly oscillating, in the spirit of the RWA.

It is noteworthy to observe that, from the perturbation theory standpoint, the last step amounts to considering additional small expansion parameters, tailored to the terms to be thrown out. For instance [21], in order to get rid of an $a^{\dagger 2}$ nonresonant term one assumes $g/2\omega$ to be of the order of λ , and for compensating an $a^{\dagger 3}\sigma$ contribution, $g/(3\omega - \varepsilon)$ should also be small. Obviously, the denominators appearing here follow the energy mismatch between the unperturbed states connected by these off-resonant terms. It becomes clear that discarding off-resonant pieces of the Hamiltonian is the same as using a multiparameter perturbative expansion.

In the literature [2] the interval [0.1,0.3] for g/ω is loosely used to identify the perturbative ultrastrong-coupling regime (pUSC) of the quantum Rabi model. In a more refined analysis [22] one finds that the pUSC region is bounded by critical coupling constants g_{pUSC} associated with the so-called Juddian points. This construction was also used to establish a spectral classification of the field-matter-coupling regimes in the QRM. On the experimental side the Bloch-Siegert shift was recently observed in strongly coupled qubit-oscillator systems [10]. An alternative improvement of the JC model relies on the Van Vleck perturbation theory to the second order in the qubit-field coupling [23].

Surprisingly, a simple analysis shows that the IBM limit is *not* recovered by the BS Hamiltonian, despite the fact that taking $\varepsilon = 0$ does not preclude the expansion parameter, now equal to g/ω , to remain small. Still, the BS model is tacitly accepted as the main candidate to describe the ultrastrong-coupling regime.

In view of this situation, in what follows we show how to obtain an effective Hamiltonian for the QRM, in the same perturbative conditions as for the BS model, i.e., up to the second order in λ , having the same simple, renormalized JC

structure and which additionally meets the test of recovering the exact IBM result for $\varepsilon = 0$.

Moreover, it will become obvious that our procedure does not rely on discarding off-resonant terms and as such it represents a *single-parameter* perturbative approach, called “perturbative” in what follows.

As the qubit energy ε approaches resonance, the spectra of the two effective models become more similar. Nevertheless, we show that important differences remain in the dressed states and are inherited by the expectation values provided by these states. Especially the excitation number turns out to be sensitive to these differences.

The rest of the paper is organized as follows. The perturbative effective Hamiltonian is derived in Sec. II. A detailed comparison of this perturbative Hamiltonian with the Bloch-Siegert model is presented and discussed in Sec. III. Their spectra, average photon number, population inversion, and number of excitations are obtained and compared both analytically and numerically in Secs. III A, III B, and III C. We also compare our result with the so-called generalized rotating-wave Hamiltonian (GRWA) obtained by Irish [24] in the deep-strong-coupling case (Sec. III D). This regime is defined by large values of the coupling, $g/\omega \approx 1$ and beyond, but the numerical evidence [25–28] shows that this approach gives good results at lower couplings too. Therefore, comparison against it is relevant. Besides, the GRWA Hamiltonian meets the IBM limit test. Section IV is left for conclusions.

II. AN IBM-COMPATIBLE EFFECTIVE HAMILTONIAN

We consider unitary transforms of the form e^S , with $S^\dagger = -S$ and their expansion in iterated commutators with their generators S . Then any operator A transforms as

$$A_S = e^S A e^{-S} = A + [S, A] + \frac{1}{2!}[S, [S, A]] + \dots \quad (3)$$

Now let us rewrite the Rabi Hamiltonian of Eq. (2) as

$$H_R = \frac{1}{2}\varepsilon\sigma_z + H_{\text{IBM}}, \quad (4)$$

in which we separate the free qubit contribution and the independent boson model part. The linear part in H_{IBM} can be absorbed in the quadratic term by a shift of the bosonic operators, produced by the generator

$$S = \lambda(a^\dagger - a)\sigma_x, \quad (5)$$

with the value of λ to be chosen later. Using

$$[S, a^\dagger] = -\lambda\sigma_x, \quad [S, a] = -\lambda\sigma_x, \quad (6)$$

it is clear that the canonical transformation amounts to a simple shift:

$$a_S^\dagger = a^\dagger - \lambda\sigma_x, \quad a_S = a - \lambda\sigma_x. \quad (7)$$

As a result, the transformed Hamiltonian becomes

$$H_{\text{IBM},S} = \omega a_S^\dagger a_S + (g - \lambda\omega)(a_S^\dagger + a_S)\sigma_x + (\lambda^2\omega - 2\lambda g). \quad (8)$$

Choosing $\lambda = g/\omega$ removes the interaction term and diagonalizes the IBM Hamiltonian:

$$H_{\text{IBM},S} = \omega a_S^\dagger a_S - g^2/\omega. \quad (9)$$

Therefore, the IBM problem alone is exactly solvable. The solution consists of the oscillator keeping its frequency ω , but shifted by g/ω , the shift direction being decided by the eigenstate of σ_x .

The presence of the free qubit part in Eq. (4) spoils this simple scenario. Both the frequency and the shift are modified, and we show below that in these circumstances a different choice for the value of λ is more appropriate.

Obviously, σ_x is left unchanged by the IBM transform. In contrast, the change in σ_z is rather complex. One can easily check that

$$\begin{aligned} [S, \sigma_z] &= -2\lambda(a^\dagger - a)i\sigma_y, \\ [S, i\sigma_y] &= -2\lambda(a^\dagger - a)\sigma_z. \end{aligned} \quad (10)$$

This means that successive commutators generate alternately the σ_z and $i\sigma_y$ operators, and each step brings in an additional factor $-2\lambda(a^\dagger - a)$. The σ_z operator collects the even terms, which add up to a hyperbolic cosine function, while the $i\sigma_y$ terms generate a hyperbolic sine function. The net result is

$$\begin{aligned} H_{R,S} &= \omega a^\dagger a + (g - \lambda\omega)(a^\dagger + a)\sigma_x + (\lambda^2\omega - 2\lambda g) \\ &+ \frac{1}{2}\varepsilon\{\cosh[2\lambda(a^\dagger - a)]\sigma_z - \sinh[2\lambda(a^\dagger - a)]i\sigma_y\}. \end{aligned} \quad (11)$$

Up to now no approximation is involved. A simpler Hamiltonian, valid to the second order in λ , is obtained by expanding $\cosh(x) \approx 1 + x^2/2$ and $\sinh(x) \approx x$. Taking into account that $\sigma_x = \sigma^\dagger + \sigma$ and $i\sigma_y = \sigma^\dagger - \sigma$, this expansion leads to an effective Hamiltonian H' of the form

$$\begin{aligned} H_{R,S} \approx H' &= \frac{1}{2}\varepsilon\sigma_z + \omega a^\dagger a + (\lambda^2\omega - 2\lambda g) \\ &+ (g - \lambda\omega + \lambda\varepsilon)(a^\dagger\sigma + a\sigma^\dagger) \\ &+ (g - \lambda\omega - \lambda\varepsilon)(a^\dagger\sigma^\dagger + a\sigma) \\ &+ \lambda^2\varepsilon(a^\dagger - a)^2\sigma_z. \end{aligned} \quad (12)$$

Now it is clear that an appropriate choice for λ is

$$\lambda = \frac{g}{\varepsilon + \omega}, \quad (13)$$

which cancels out the off-resonant term linear in the bosonic operators. This is the same small parameter as the one used in the Bloch-Siegert formalism [21]. The effective Hamiltonian has now the expression

$$\begin{aligned} H' &= \frac{1}{2}\varepsilon\sigma_z + \omega a^\dagger a - (2\lambda g - \lambda^2\omega) \\ &+ 2\lambda\varepsilon(a^\dagger\sigma + a\sigma^\dagger) + \lambda^2\varepsilon(a^\dagger - a)^2\sigma_z. \end{aligned} \quad (14)$$

Finally, one has to handle the last, quadratic term. To this end one considers a second unitary transform, with the generator

$$S' = \frac{1}{2}\eta(a^{\dagger 2} - a^2)\sigma_z. \quad (15)$$

This σ_z -dependent squeezing transform [29] leads to

$$[S', a^\dagger] = -\eta a\sigma_z, \quad [S', a] = -\eta a^\dagger\sigma_z, \quad (16)$$

in which again successive commutators generate alternately the same two operators. One gets a Bogolyubov-type

transform:

$$\begin{aligned} a_{S'}^\dagger &= \cosh \eta a^\dagger - \sinh \eta a\sigma_z, \\ a_{S'} &= -\sinh \eta a^\dagger\sigma_z + \cosh \eta a. \end{aligned} \quad (17)$$

Different Hamiltonian pieces change accordingly, for instance, the photon number operator

$$\begin{aligned} a_{S'}^\dagger a_{S'} &= \cosh 2\eta a^\dagger a + \sinh^2 \eta \\ &- \frac{1}{2} \sinh 2\eta (a^\dagger - a)^2\sigma_z - \frac{1}{2} \sinh 2\eta (2a^\dagger a + 1)\sigma_z \end{aligned} \quad (18)$$

and

$$\begin{aligned} (a_{S'}^\dagger - a_{S'}) &= (\cosh \eta + \sinh \eta\sigma_z)(a^\dagger - a), \\ (a_{S'}^\dagger - a_{S'})^2\sigma_z &= [\cosh 2\eta\sigma_z + \sinh 2\eta](a^\dagger - a)^2. \end{aligned} \quad (19)$$

From Eqs. (18) and (19) above the quantities in $H'_{S'}$ containing $(a^\dagger - a)^2$ are identified as

$$X_z := \sigma_z \left(\lambda^2\varepsilon \cosh 2\eta - \frac{\omega}{2} \sinh 2\eta \right) (a^\dagger - a)^2, \quad (20)$$

$$X_0 := \lambda^2\varepsilon \sinh 2\eta (a^\dagger - a)^2. \quad (21)$$

The terms contained in X_z cancel out by choosing η so that

$$\frac{1}{2} \sinh 2\eta = \frac{\lambda^2\varepsilon}{\omega} \cosh 2\eta. \quad (22)$$

The condition makes η of second order in λ and, neglecting higher contributions, one has

$$\eta = \frac{\lambda^2\varepsilon}{\omega}. \quad (23)$$

In this case the term X_0 in Eq. (21) is of fourth order in λ and is discarded.

The terms in the Hamiltonian equation (14) not considered up to now are the free qubit energy, which commutes with S' , and the JC interaction $2\lambda\varepsilon(a^\dagger\sigma + a\sigma^\dagger)$, which is already a first-order quantity, and therefore, its transformation by $S' \sim \lambda^2$ brings in changes of at least third order. Therefore, both are kept unchanged.

Finally, expanding systematically the hyperbolic functions to second order in λ (i.e., first order in η) and spelling out the expressions of λ and η in terms of the model parameters, leaves us with $H'_{S'} \approx H_P$ where the perturbative IBM-compatible effective Hamiltonian is given by

$$\begin{aligned} H_P &= \frac{\varepsilon}{2} \left(1 - \frac{2g^2}{(\varepsilon + \omega)^2} \right) \sigma_z + \left(\omega - \frac{2g^2\varepsilon}{(\varepsilon + \omega)^2} \sigma_z \right) a^\dagger a \\ &+ 2 \frac{g\varepsilon}{\varepsilon + \omega} (a^\dagger\sigma + a\sigma^\dagger) - \frac{g^2}{\varepsilon + \omega} \frac{2\varepsilon + \omega}{\varepsilon + \omega}. \end{aligned} \quad (24)$$

This expression of the effective Hamiltonian H_P is the main result of the paper.

It is now obvious that for $\varepsilon = 0$, H_P recovers exactly the IBM result, Eq. (9), and moreover, this holds for all values of the coupling constant g .

III. COMPARING EFFECTIVE HAMILTONIANS

The main difference between the present approach and the BS one [21] is seen in the choice of the first unitary

transform. For the perturbative derivation of the BS effective Hamiltonian one uses the generator

$$\tilde{S} = \lambda(a^\dagger \sigma^\dagger - a\sigma). \quad (25)$$

This choice is aimed at diagonalizing the off-resonant interaction in H_R . In contrast, we employed a Lang-Firsov generator, Eq. (5), which changes both the resonant and the off-resonant interaction. A second transform becomes necessary here too, to remove terms of the second order in the bosonic operators. Its generator has the same expression, Eq. (15), but with the strength $\eta = \lambda g/\omega$, assumed to be of the order λ^2 .

Finally, one keeps in the resulting expansion terms up to the second order in λ and discards highly nonresonant ones, like, e.g., $a^3 \sigma^\dagger$, which are generated in the process.

The resulting Bloch-Siegert and the perturbative effective Hamiltonian given by Eq. (24) both have the structure of a renormalized JC model:

$$H = \frac{1}{2}(\varepsilon + \Omega)\sigma_z + (\omega + \Omega\sigma_z)a^\dagger a + \gamma(a^\dagger \sigma + a\sigma^\dagger) - \delta. \quad (26)$$

The difference comes from the parameters Ω , γ , and δ . They are given by [22]

$$\Omega = \frac{g^2}{\omega + \varepsilon}, \quad \gamma = g, \quad \delta = \frac{1}{2} \frac{g^2}{\omega + \varepsilon} \quad (27)$$

for $H = H_{BS}$ and by

$$\Omega = -\frac{g^2}{\omega + \varepsilon} \frac{2\varepsilon}{\omega + \varepsilon}, \quad \gamma = g \frac{2\varepsilon}{\omega + \varepsilon}, \quad \delta = \frac{g^2}{\omega + \varepsilon} \frac{\omega + 2\varepsilon}{\omega + \varepsilon} \quad (28)$$

for $H = H_P$.

The JC structure of Eq. (26) reduced the problem to 2×2 blocks, indexed by the photon number n . In the corresponding basis $\{|n, \uparrow\rangle, |n+1, \downarrow\rangle\}$ the n th block has the form

$$\begin{aligned} \hat{h}_n &= \alpha_n \sigma_0 + \frac{1}{2} \Delta_n \sigma_z + \gamma \sqrt{n+1} \sigma_x \\ &= \alpha_n \sigma_0 + R_n (\cos \theta_n \sigma_z + \sin \theta_n \sigma_x), \end{aligned} \quad (29)$$

where σ_0 is the 2×2 unit matrix and we introduce

$$\alpha_n = \omega(n+1/2) - \left(\frac{\Omega}{2} + \delta \right), \quad (30)$$

$$R_n = \sqrt{\Delta_n^2/4 + \gamma^2(n+1)}, \quad (31)$$

with $\Delta_n = \varepsilon - \omega + 2\Omega(n+1)$ acting as an effective, n -dependent detuning. The angle θ_n is defined by the relations $\cos \theta_n = \Delta_n/(2R_n)$ and $\sin \theta_n = \gamma \sqrt{n+1}/R_n$. Note that $\Omega/2 + \delta$ turns out to take the same value $g^2/(\omega + \varepsilon)$ in both effective Hamiltonians considered; therefore, the middle points of their spectra coincide.

It is known that the spectrum of \hat{h}_n is $E_{n,\pm} = \alpha_n \pm R_n$ with the eigenvectors (i.e., dressed states) given by the linear combination

$$|\varphi_{n,\pm}\rangle := u_\pm |n, \uparrow\rangle + v_\pm |n+1, \downarrow\rangle, \quad (32)$$

where $(u_+, v_+) = (\cos \theta_n/2, \sin \theta_n/2)$ for the higher state $|\varphi_{n,+}\rangle$ and $(u_-, v_-) = (\sin \theta_n/2, -\cos \theta_n/2)$ for the lower state $|\varphi_{n,-}\rangle$. To complete the picture we also calculated the energy of the ground state $|0, \downarrow\rangle$ as $E_0 = -\varepsilon/2 - (\Omega/2 + \delta)$.

By examining Eqs. (27) and (28), it is clear that the differences between the two models are more pronounced for small

values of ε . As already mentioned, at $\varepsilon = 0$, H_P recovers the exact IBM result, while H_{BS} does not.

On the other hand at resonance, $\varepsilon = \omega$, the parameters of the two models coincide, *except for the sign of Ω* . The latter has no bearing on the spectra, which therefore are the same for the two models, but it modifies the structure of the eigenstates. Indeed, at resonance the sign of Ω carries over to a sign change in $\cos \theta_n$ which in turn leads to interchanging $\cos \theta_n/2$ and $\sin \theta_n/2$. In other words, even though at resonance the spectra of H_{BS} and H_P coincide, because of the sign difference in Δ_n the attribution of the eigenvalues is flipped: for example, the weight of the two basis vectors $|n, \uparrow\rangle$ and $|n+1, \downarrow\rangle$ in the upper state $|\varphi_{n,+}\rangle$ of the BS Hamiltonian is the same as for the lower state $|\varphi_{n,-}\rangle$ of the perturbative Hamiltonian. Further consequences of this fact are analyzed in Sec. III C.

To resume the situation, the two models predict different spectra and states, as suggested by these two examples. Intermediate values for $\varepsilon \in [0, \omega]$ are expected to lead to similar conclusions. Let us also remark that Ω is interpreted as a bosonic frequency shift which depends on the qubit state, and detecting the former gives information about the latter [2]. Therefore, the sign difference means that this way of reading the qubit state works in opposite directions in the predictions of the two models.

Still, these arguments are merely heuristic. Eigenstates are not directly comparable, H_P and H_{BS} having been obtained by different unitary transforms; i.e., the two effective Hamiltonians work in different bases. The relevant comparison is on basis-independent quantities, to which we turn below.

A. Energy spectra

At resonance, $\varepsilon = \omega$, all parameters in Eq. (29) are exactly the same for the two cases, except for sign of Δ_n , and thus the spectra are identical. On the other hand, in the limit $\varepsilon = 0$, H_P becomes exact. Therefore, it is expected that for the whole subresonant range, $\varepsilon \leq \omega$, our approach is an improvement over the BS effective Hamiltonian.

To illustrate this fact we compare in Fig. 1 the spectra of the two effective models (BS and perturbative) and those produced by numerical diagonalization of the full Rabi Hamiltonian. For the latter a cutoff at $N_{ph} = 30$ photons is found to be sufficient. We use $\omega = 1$ units throughout, since the problem is homogeneous of degree 1 in the parameters; i.e., it is defined essentially by only two dimensionless parameters ε/ω and g/ω . Henceforth the coupling constant g and all energies are given in units of ω .

We selected the pair of spectral branches $E_{4,\pm}$ for three values of the qubit energy ε . However, in the IBM limit [i.e., for $\varepsilon = 0$, see Fig. 1(a)] two additional branches are added to illustrate that the coinciding spectra of the Rabi and perturbative Hamiltonians are doubly degenerate, while the Bloch-Siegert spectrum displays a degeneracy lifting as the qubit-photon coupling strength increases. Note that for the sake of clarity the spectral branches of H_R are represented by red circles.

To understand these differences one has to recall that in the limit $\varepsilon = 0$, H_P becomes exact, while the BS spectra are

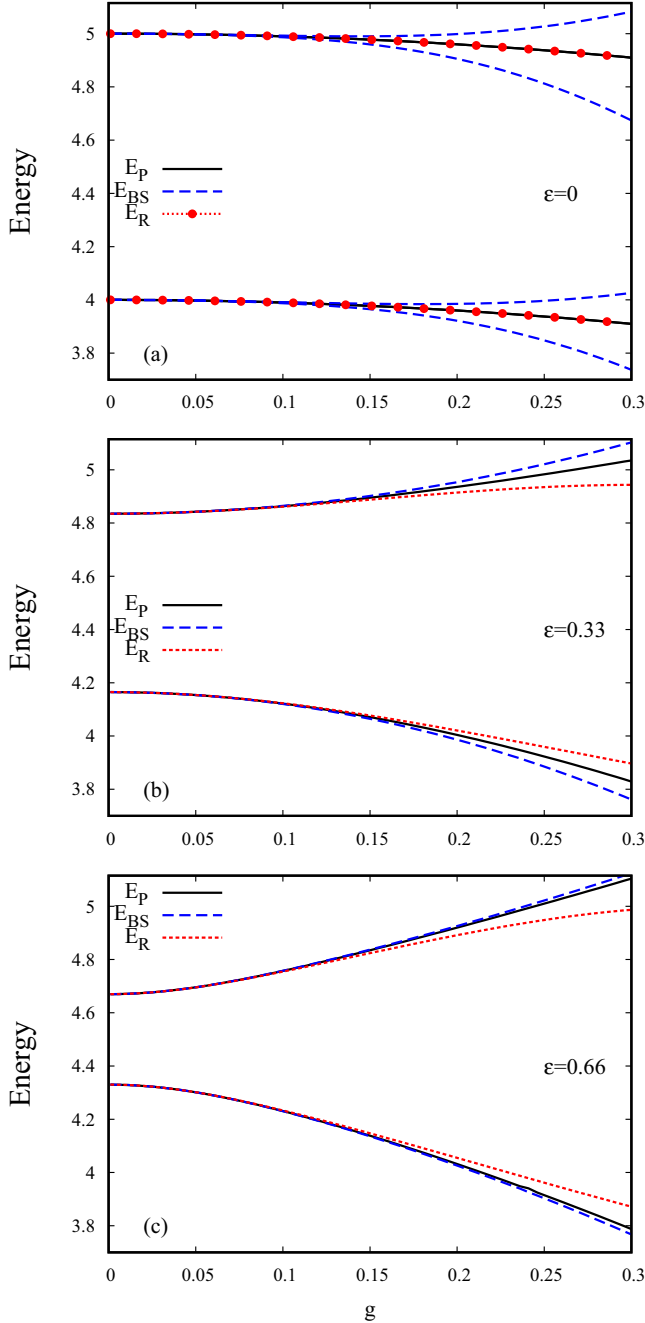


FIG. 1. Two spectral branches of the Rabi (R), Bloch-Siegert (BS), and perturbative (P) Hamiltonians as a function of the matter-photon coupling g at different values of the qubit energy: (a) $\varepsilon = 0$, (b) $\varepsilon = 0.33$, and (c) $\varepsilon = 0.66$. The spectrum of the QRM is calculated numerically. g is restricted to the perturbative USC regime. Panel (a) also includes the branches $E_{3,+}$ and $E_{5,-}$ (see the text). The coupling constant g and the energy are given in units of ω .

correct only to λ^2 accuracy, as it is easy to check on the expression for $E_{n,\pm}$. With increasing ε the spectral difference between the models diminishes [see Figs. 1(b) and 1(c)], as predicted by the analytic expression of H_P and H_{BS} until for $\varepsilon = 1$ they coincide (not shown). In the process the perturbative values remain closer to the exact Rabi result than the BS ones.

B. Operator averages: Photon population

When calculating the expectation value of an operator on a given eigenstate of the effective Hamiltonian, one has to take into account the unitary transforms that lead to it. The operators should be “rotated” by the same procedure as the Hamiltonian.

In the case of H_P , we use again the two generators $S = \lambda(a^\dagger - a)\sigma_x$ and $S' = \frac{1}{2}\eta(a^{\dagger 2} - a^2)\sigma_z$, with the parameters given in Eqs. (13) and (23). The observable we are interested in is the photon number $\hat{n} = a^\dagger a$. From Eq. (7) we obtain by the first transform

$$a_S^\dagger a_S = a^\dagger a - \lambda(a^\dagger + a)\sigma_x + \lambda^2. \quad (33)$$

The second step involves S' and is apparently more complicated but it gets simpler by limiting the expansion to second order in λ and taking into account that $\eta \sim \lambda^2$. For instance, it is clear that the second term in Eq. (33) remains unchanged. Indeed, changes are at least of first power of η and with the prefactor λ they are third-order quantities.

For the first term $a^\dagger a$ one uses Eq. (18) expanded to second order in λ , with the net result that after both transforms one has

$$\hat{n}_{S,S'} \approx \hat{n} - \eta(a^{\dagger 2} + a^2)\sigma_z - \lambda(a^\dagger + a)\sigma_x + \lambda^2. \quad (34)$$

This is the operator to be averaged on the eigenstates of the form given in Eq. (32). Things turn out to be further simplified by noting that operators like a^2 and $a\sigma$ and their hermitic conjugates do not contribute to the expectation value, since they do not connect vectors belonging to the same two-dimensional subspace.

To conclude, one has

$$\begin{aligned} \langle \hat{n} \rangle_{P,\pm} &= \langle \varphi_{n,\pm} | [a^\dagger a - \lambda(a^\dagger \sigma + a \sigma^\dagger) + \lambda^2] | \varphi_{n,\pm} \rangle \\ &= u_\pm^2 n + v_\pm^2 (n+1) - 2\lambda u_\pm v_\pm \sqrt{n+1} + \lambda^2, \end{aligned} \quad (35)$$

where the index P recalls that the average is calculated with respect to the dressed states of H_P . Obviously, $\langle \hat{n} \rangle_{P,\pm}$ depends on the specific two-dimensional subspace n as well, but we drop this additional index for the simplicity of writing. Replacing u_\pm and v_\pm leads to the values

$$\langle \hat{n} \rangle_{P,\pm} = n + \frac{1}{2}(1 \mp \cos \theta_n) \mp \lambda \sin \theta_n \sqrt{n+1} + \lambda^2. \quad (36)$$

A negative sign of Ω means a lower $\cos \theta_n$ value, and this encourages a higher photon population in the upper state. For the ground state one obtains $\langle \hat{n} \rangle_{P,0} = \lambda^2$.

The prediction of the Bloch-Siegert Hamiltonian for the same quantity is evaluated by the same procedure. Some differences arise though, beginning with the first generator \tilde{S} of Eq. (25) with the result that now

$$a_S^\dagger a_S = a^\dagger a - \lambda(a^\dagger \sigma^\dagger + a \sigma) + \lambda^2 \sigma \sigma^\dagger - \lambda^2 a^\dagger a \sigma_z. \quad (37)$$

The second transform has the same form $\tilde{S}' = \frac{1}{2}\eta(a^{\dagger 2} - a^2)\sigma_z$, with $\eta \sim \lambda^2$.

As before, the terms containing λ remain unchanged up to the second order, and the first term $a^\dagger a$ is modified by a combination of a^2 and $a^{\dagger 2}$, which do not contribute to the expectation value. The new feature is that no contribution comes from the second term in Eq. (37) above. Therefore, one

is led to

$$\begin{aligned} \langle \hat{n} \rangle_{\text{BS},\pm} &= \langle \varphi_{n,\pm} | [a^\dagger a + \lambda^2 \sigma \sigma^\dagger - \lambda^2 a^\dagger a \sigma_z] | \varphi_{n,\pm} \rangle \\ &= u_\pm^2 (n - \lambda^2 n) + v_\pm^2 [n + 1 + \lambda^2 (n + 2)]. \end{aligned} \quad (38)$$

As a result one has

$$\langle \hat{n} \rangle_{\text{BS},\pm} = n + \frac{1}{2} + \lambda^2 \mp \left(\frac{1}{2} + \lambda^2 (n + 1) \right) \cos \theta_n. \quad (39)$$

For the ground state one finds $\langle \hat{n} \rangle_{\text{BS},0} = \lambda^2$.

The numerical results presented in Fig. 2 complement our analysis. We calculated the mean photon number N corresponding to the eigenstates of the fourth two-dimensional Jaynes-Cummings subspace for the exact and the effective Hamiltonians. Again, we find that in the IBM limit [see Fig. 2(a)] the perturbative Hamiltonian reproduces the exact expectation value of the Rabi model (again, we used red circles to highlight the results of the exact model). Note that for $\varepsilon = 0$ one has $S' = 0$ too. Thus one is left with only the first transform Eq. (33), which is exact. Thus, not only the Hamiltonian but also the “rotated” form of the \hat{n} operator is exact. In contrast, the results obtained from the Bloch-Siegert model show noticeable differences starting around the qubit-photon coupling strength $g \sim 0.15$. In particular, the mean photon number corresponding to $|\varphi_{4,+}\rangle$ decreases as g increases [see the upper curve in Fig. 2(a)]. These differences are even more pronounced for higher two-dimensional subspaces. As in the case of the spectrum, the photon number expectation values given by the two models become closer as ε increases, with the perturbative ones remaining nearer to the exact Rabi values [see Figs. 2(b) and 2(c)].

C. Operator averages: Population inversion and number of excitations

More clear-cut differences exist between the two models than suggested by the above results, especially at resonance. We show this by performing the same comparison of expectation values, this time for the population inversion operator σ_z and for the number of excitations $\hat{N}_x = \hat{n} + 1/2(1 + \sigma_z)$.

For H_P the change of σ_z under the first unitary transform is obtained as in the derivation of Eqs. (10) and (11):

$$\begin{aligned} \sigma_{z,S} &= \cosh[2\lambda(a^\dagger - a)]\sigma_z - \sinh[2\lambda(a^\dagger - a)]i\sigma_y \\ &\approx \sigma_z + 2\lambda^2(a^\dagger - a)^2\sigma_z - 2\lambda(a^\dagger - a)i\sigma_y. \end{aligned} \quad (40)$$

The expression remains unchanged by the second transform, which commutes with σ_z . The terms containing λ are left unchanged, as discussed in the previous cases. Also, as before, the operators a^2 and $a^{\dagger 2}$ and the off-resonant ones $a^\dagger \sigma^\dagger$ and $a \sigma$ do not contribute to the expectation value. We are left with

$$\sigma_{z,S,S'} = \sigma_z + 2\lambda(a^\dagger \sigma + a \sigma^\dagger) - 2\lambda^2(2a^\dagger a + 1)\sigma_z, \quad (41)$$

which by straightforward calculations leads to

$$\begin{aligned} \langle \sigma_z \rangle_{\text{P},\pm} &= (u_\pm^2 - v_\pm^2)[1 - 2\lambda^2(2n + 1)] \\ &\quad + 4\lambda u_\pm v_\pm \sqrt{n + 1} + 4\lambda^2 v_\pm^2. \end{aligned} \quad (42)$$

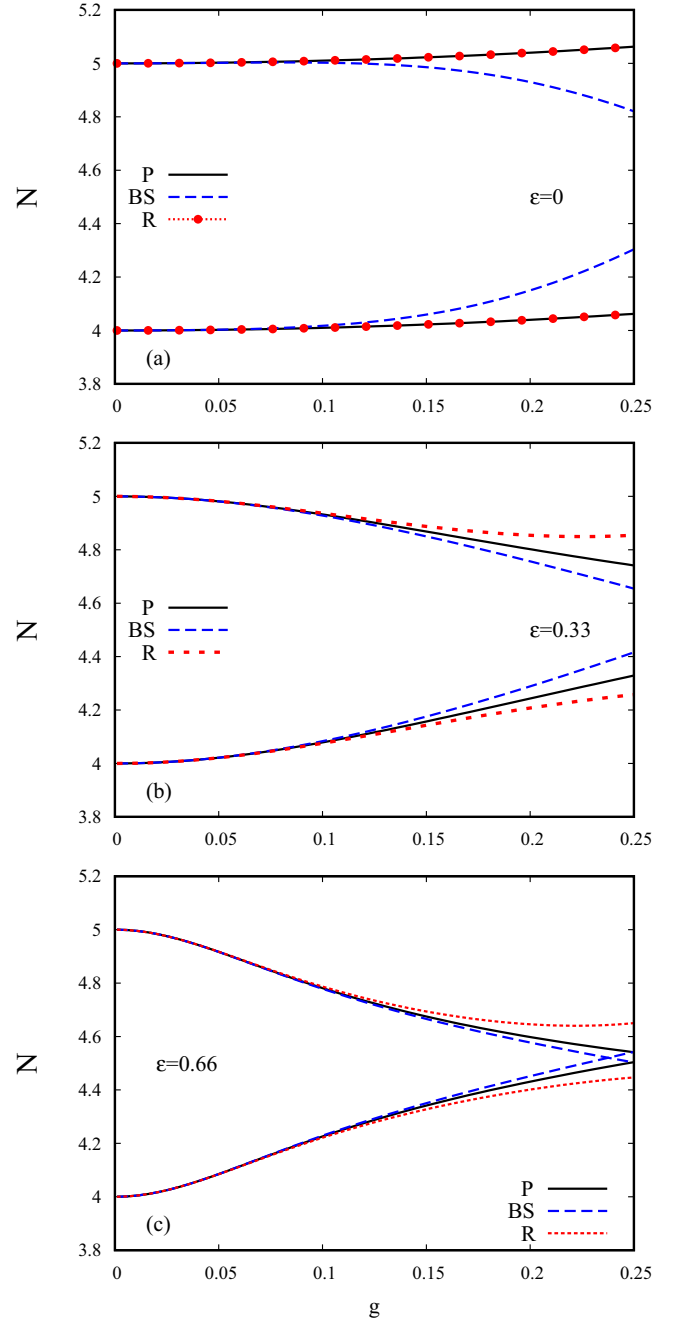


FIG. 2. The mean photon number N associated with the eigenstates $|\varphi_{4,\pm}\rangle$ of the Rabi (R), Bloch-Siegert (BS), and perturbative (P) Hamiltonians as a function of the matter-photon coupling g at different values of the qubit energy: (a) $\varepsilon = 0$, (b) $\varepsilon = 0.33$, and (c) $\varepsilon = 0.66$.

Specifically for the two states one obtains

$$\begin{aligned} \langle \sigma_z \rangle_{\text{P},\pm} &= \pm \cos \theta_n [1 - 4\lambda^2 (n + 1)] \\ &\quad \pm 2\lambda \sin \theta_n \sqrt{n + 1} + 2\lambda^2. \end{aligned} \quad (43)$$

A negative value for $\cos \theta_n$ hints to a higher population inversion on the lower state. For the ground state one finds $\langle \sigma_z \rangle_{\text{P},0} = -1 + 2\lambda^2$.

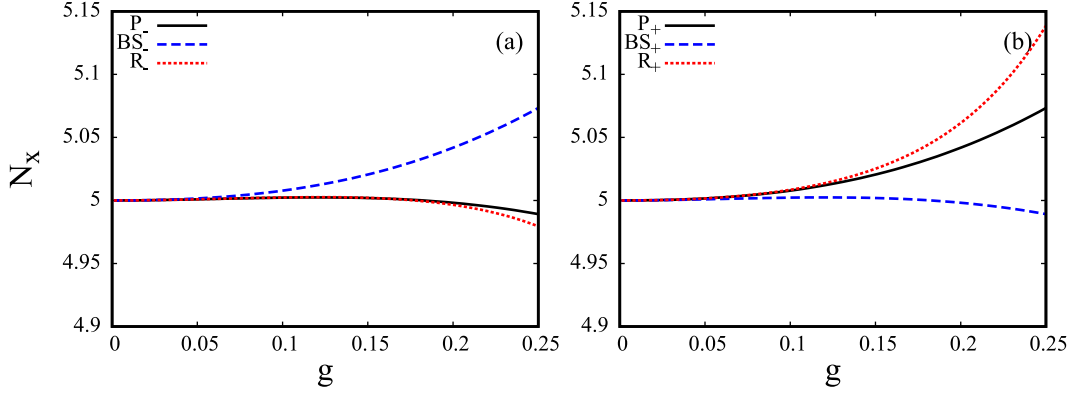


FIG. 3. Two branches of the number of excitations N_x^\pm associated with the pair of dressed states $|\varphi_{4,\pm}\rangle$ as a function of the qubit-photon coupling strength g in the resonant regime $\varepsilon = 1$. (a) N_x^- , the expectation value of the excitation number for the lower spectral branch. (b) N_x^+ , the same for the upper spectral branch. The obvious similarity between the results of the Rabi and the perturbative models confirms the correct assignment of N_x^\pm to the upper and lower spectral branches.

Finally, we address the same problem for H_{BS} . The transform of σ_z under $\tilde{S} = \lambda(a^\dagger\sigma^\dagger - a\sigma)$ is complicated, but for the second order in λ the quantities $[\tilde{S}, \sigma_z]$ and $[\tilde{S}, [\tilde{S}, \sigma_z]]$ are sufficient. It is easy to check that

$$\begin{aligned} [\tilde{S}, \sigma_z] &= -2\lambda(a^\dagger\sigma^\dagger + a\sigma), \\ [\tilde{S}, a^\dagger\sigma^\dagger + a\sigma] &= 2\lambda(a^\dagger a\sigma_z - \sigma\sigma^\dagger). \end{aligned} \quad (44)$$

This leads to the result

$$\sigma_{z,\tilde{S}} = \sigma_z - 2\lambda(a^\dagger\sigma^\dagger + a\sigma) - 2\lambda^2(a^\dagger a\sigma_z - \sigma\sigma^\dagger), \quad (45)$$

which remains unchanged under the second unitary transform. Thus

$$\begin{aligned} \langle\sigma_z\rangle_{BS,\pm} &= \langle\varphi_{n,\pm}|[\sigma_z - 2\lambda^2(a^\dagger a\sigma_z - \sigma\sigma^\dagger)]|\varphi_{n,\pm}\rangle \\ &= (u_\pm^2 - v_\pm^2)(1 - 2\lambda^2 n) + 4\lambda^2 v_\pm^2. \end{aligned} \quad (46)$$

Specifically, for the two states one has

$$\begin{aligned} \langle\sigma_z\rangle_{BS,\pm} &= \pm \cos\theta_n(1 - 2\lambda^2 n) + 2\lambda^2(1 \mp \cos\theta_n) \\ &= \pm \cos\theta_n[1 - 2\lambda^2(n+1)] + 2\lambda^2. \end{aligned} \quad (47)$$

For the ground state one finds $\langle\sigma_z\rangle_{BS,0} = -1 + 2\lambda^2$.

The average of the operator \hat{N}_x is now easily done for both effective Hamiltonians by assembling Eqs. (36), (39), (43), and (47). The surprising result is that the outcome is the same for both effective models and reads

$$N_x^\pm = \langle\varphi_{n,\pm}|\hat{N}_x|\varphi_{n,\pm}\rangle = n + 1 + 2\lambda^2 \mp 2\lambda^2(n+1)\cos\theta_n. \quad (48)$$

This is not a mere coincidence and relies essentially on the fact that the generators of the respective unitary transforms differ by $\tilde{S} := S - \tilde{S} = \lambda(a^\dagger\sigma - a\sigma^\dagger)$, which commutes with \hat{N}_x [30].

Again, the interesting situation is provided by the resonant case. There one can see analytically that both models predict exactly the same results for a given spectral subspace. The curves for N_x^\pm are superimposed since, except for the sign, the cosine values coincide. But because of this sign difference, inherited from the opposite signs of Ω_P and Ω_{BS} , the assignment of N_x expectation values to the energy branches is switched, $N_{x,BS}^\pm = N_{x,P}^\mp$. More precisely, in the BS model

N_x^- , corresponding to the lower branch, takes the higher value, while N_x^+ , stemming from the upper branch, is smaller. In the perturbative case, it is the other way around. This is an important difference, expressing the distinct structure of the eigenstates, and which cannot gradually disappear as λ gets smaller. To decide which attribution is the correct one we rely on comparison with the result of the full Rabi Hamiltonian.

The outcome is shown in Fig. 3, in which the values of the two models are plotted, along with the numerical calculation using the dressed states provided by diagonalization of the Rabi Hamiltonian. Figure 3(a) corresponds to the eigenstates $|\varphi_{4,-}\rangle$ and the Fig. 3(b) corresponds to $|\varphi_{4,+}\rangle$. One can check by inspection of Figs. 3(a) and 3(b) that $N_{x,P}^\pm = N_{x,BS}^\mp$ and that comparison with the Rabi solutions decides in favor of the perturbative results.

Finally we compare in Fig. 4 the number of excitations for the same values of the qubit energy considered in previous discussions. In the IBM limit $N_{x,P}^\pm$ follow qualitatively the exact curves but also deviate from them as g increases. (Let us stress that for $\varepsilon = 0$ the exact result is analytically available in terms of Laguerre polynomials [16], but here we stick to Eq. (48), in which the operators are rotated only to second order.) On the other hand, the excitation numbers of the BS model are quite far from $N_{x,R}^\pm$ for all values of ε . In particular, at $\varepsilon = 0.66$ the branches of $N_{x,BS}^\pm$ exhibit an incorrect crossing point around $g = 0.235$. Moreover, the BS attribution of the excitation number to a given spectral branch is still flipped and the inequality $N_{x,BS}^+ < N_{x,BS}^-$ still holds. On the contrary, the branches $N_{x,P}^\pm$ follow closely the exact ones in the subresonant regime too.

D. The generalized RWA effective Hamiltonian

A successful effective Hamiltonian suitable in the deep-strong-coupling (DSC) regime defined by $g/\omega \geq 1$ [2] was proposed by Irish [24]. This so-called generalized RWA (GRWA) Hamiltonian follows from H_R [see Eq. (2)] by the IBM transform. The free qubit part of the Hamiltonian then couples all pairs of shifted oscillator states.

To be specific, the model uses a single canonical transform, generated by $S = \lambda(a^\dagger - a)\sigma_x$, this time with $\lambda = g/\omega$. As a

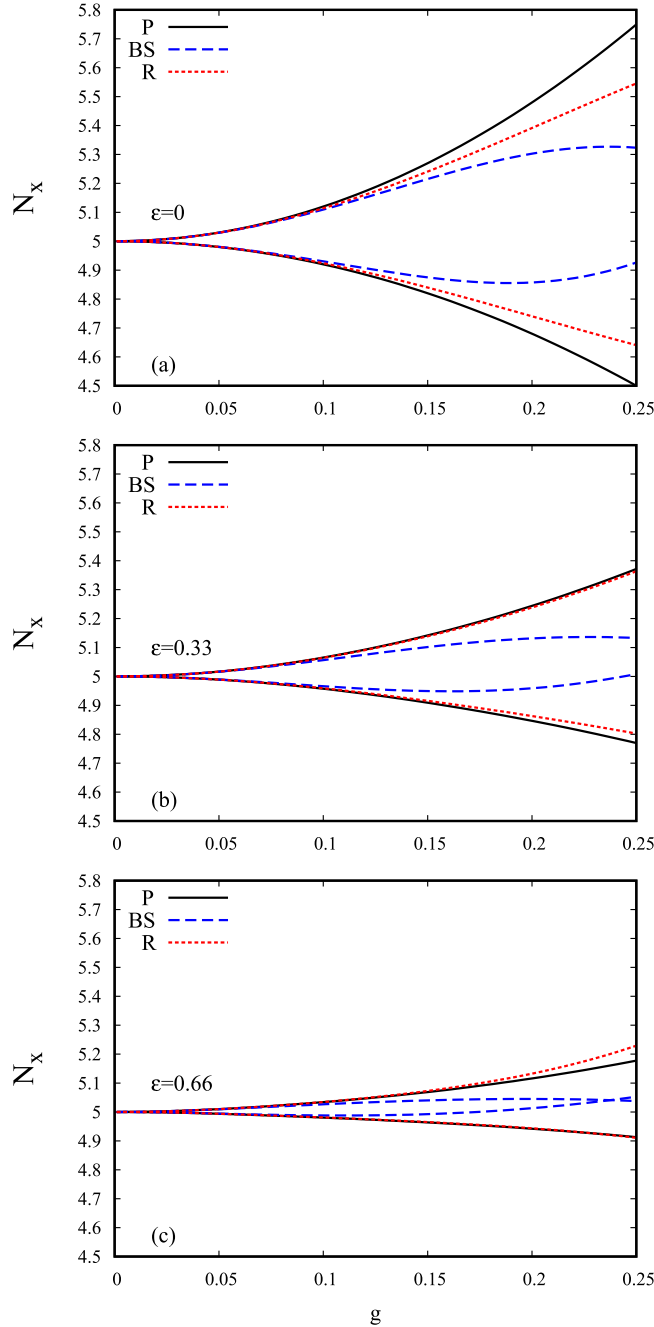


FIG. 4. The number of excitations N_x associated with the pair of dressed states in the fourth spectral subspace as a function of the field-matter coupling strength g , for the perturbative (P), Bloch-Siegert (BS), and Rabi (R) Hamiltonians. The IBM limit $\varepsilon = 0$ (a), $\varepsilon = 0.33$ (b), and $\varepsilon = 0.66$ (c).

result one obtains, as for Eq. (11),

$$H_{R,S} = \omega a^\dagger a - g^2/\omega + \frac{1}{2}\varepsilon\{\cosh[2\lambda(a^\dagger - a)]\sigma_z - \sinh[2\lambda(a^\dagger - a)]i\sigma_y\}. \quad (49)$$

It is lengthy but rather straightforward to expand the hyperbolic functions as the even and odd parts of the exponential

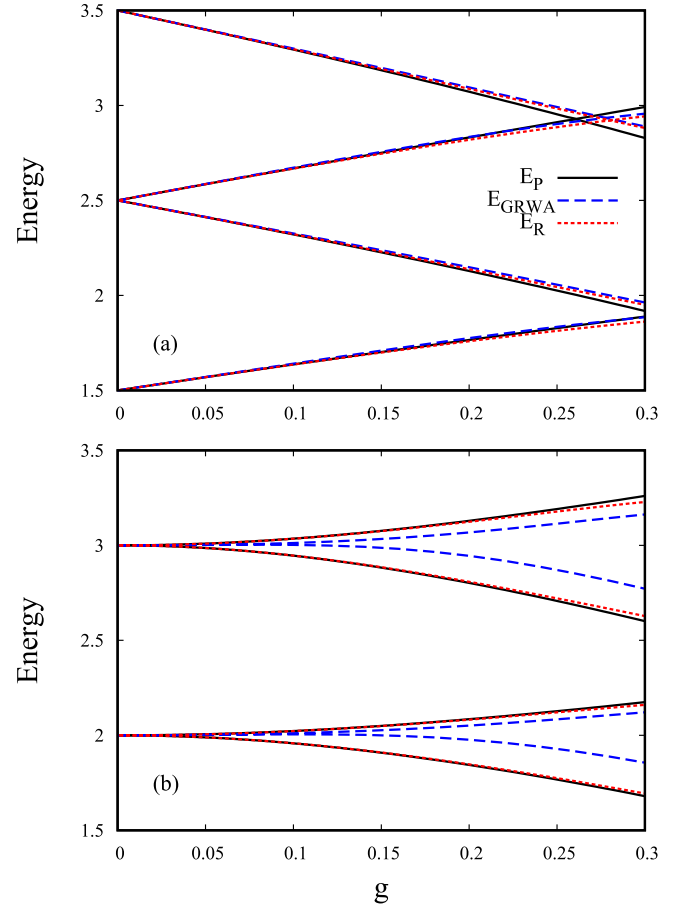


FIG. 5. Several spectral branches of the Rabi (R), GRWA, and perturbative (P) Hamiltonians as a function of the matter-photon coupling g in the (a) resonant regime $\varepsilon = 1$ and the (b) supraperturbative regime $\varepsilon = 2$. g is restricted to the perturbative USC regime.

(see Xie *et al.* [26])

$$e^{2\lambda(a^\dagger - a)} = f_0(\hat{n}, \lambda) + \sum_{q>0} [a^{\dagger q} f_q(\hat{n}, \lambda) + (-1)^q f_q(\hat{n}, \lambda) a^q], \quad (50)$$

where the functions of \hat{n} are defined, as usual, by their action on the elements of the Fock basis $f_q(\hat{n}, \lambda) |n\rangle = f_q(n, \lambda) |n\rangle$. They are related to the generalized Laguerre polynomials $L_n^{(q)}(x)$ by

$$f_q(n, \lambda) = e^{-2\lambda^2} (2\lambda)^q \frac{n!}{(n+q)!} L_n^{(q)}(4\lambda^2). \quad (51)$$

This translates into the following expression for $H_{R,S}$

$$H_{R,S} = \omega a^\dagger a - g^2/\omega + \frac{\varepsilon}{2} f_0(\hat{n}, \lambda) \sigma_z + \frac{\varepsilon}{2} \sum_{q>0, \text{even}} [a^{\dagger q} f_q(\hat{n}, \lambda) + f_q(\hat{n}, \lambda) a^q] \sigma_z + \frac{\varepsilon}{2} \sum_{q>0, \text{odd}} [a^{\dagger q} f_q(\hat{n}, \lambda) - f_q(\hat{n}, \lambda) a^q] (\sigma - \sigma^\dagger). \quad (52)$$

No approximation is involved so far. The f_0 term is diagonal, while terms with higher q values are further away from the diagonal in the Fock basis.

The idea of the GRWA is to keep, besides the diagonal terms, only the off-diagonal ones with $q = 1$ and which, moreover, are also retained in the RWA as not counter-rotating. More precisely, one has

$$H_{\text{GRWA}} = \omega a^\dagger a - g^2/\omega + \frac{\epsilon}{2} f_0(\hat{n}, \lambda) \sigma_z + \frac{\epsilon}{2} [a^\dagger \sigma f_1(\hat{n}, \lambda) + f_1(\hat{n}, \lambda) a \sigma^\dagger], \quad (53)$$

which reduces the Hamiltonian to the familiar JC structure, renormalized by \hat{n} -dependent factors. Thus the problem becomes 2×2 block diagonal and therefore solvable.

Obviously, this approach is not a systematic expansion to λ^2 . Indeed, $f_q \sim \lambda^q$ and therefore terms with f_2 should have been kept as second-order contributions. Instead they were discarded as off-resonant, as prescribed by the RWA argument.

The success of the model in the DSC regime relies on the fact that *all* terms arising from the transformed qubit energy become small at large g , due to the exponential prefactor. Surprisingly, its predictions work quite well at lower couplings too. This means that at least in certain circumstances the off-resonant terms are negligible indeed. On the contrary, in situations like $\epsilon \approx 2\omega$ this is not the case any more. Terms like $a^{\dagger 2} \sigma$ now describe resonant transitions in the system and thus are no longer negligible. In contrast, these processes are included in the present perturbative approach by its second unitary transform S' .

The situation is illustrated in Fig. 5 where we compare a part of the low-energy spectra of the Rabi, GRWA, and perturbative Hamiltonians in the resonant ($\epsilon = \omega$) and supracritical ($\epsilon > \omega$) regimes. The eigenvalues of the GRWA Hamiltonian [24] are given analytically by Eq. (53). Clearly, the eigenvalues of both GRWA and perturbative Hamiltonians reasonably follow the Rabi spectrum in the resonant case along the whole range of the pUSC regime [see Fig. 5(a)]. However, Fig. 5(b) reveals that in the supracritical regime the GRWA spectrum is no longer accurate in the pUSC regime while the errors of the perturbative model are quite small.

IV. CONCLUSIONS

The effective Hamiltonian given by Eq. (24) was derived from the quantum Rabi model systematically to second order in the small parameter $\lambda = g/(\epsilon + \omega)$. No other approximations (like discarding terms as off-resonant) are involved. The expansion parameter λ is the same as in the Bloch-Siegert theory. In contrast to the latter, the present formalism recovers exactly the IBM Hamiltonian in the limit $\epsilon \rightarrow 0$. The proposed model allows analytical calculations of various operator averages which are used for a detailed comparison with the predictions of the BS approach.

In Secs. III A–III C, we compared the exact Rabi model to the predictions of the two effective Hamiltonians over the range $g/\omega \in [0, 0.25]$ and for several fixed values of the qubit energy ϵ . The increased accuracy of the IBM-compatible effective Hamiltonian is confirmed in various regimes. Two special cases are particularly significant.

(i) In the IBM limit, $\epsilon = 0$, our effective Hamiltonian reproduces the energy spectrum and the mean photon number of the exact Rabi model, while the BS Hamiltonian displays an incorrect splitting in the spectrum and substantial deviations of the mean photon number.

(ii) In the resonant case, $\epsilon = \omega$, when the spectra of the two models coincide, the difference is seen in the structure of the dressed eigenstates. The source of this dissimilarity is traced back to the different sign of the frequency shift induced by the qubit-field coupling. This is further reflected in the expectation values of relevant observables, like the excitation number, and their attribution to the appropriate eigenstates.

Therefore, it is natural to expect that in the intermediate, subresonant regime, $0 < \epsilon < \omega$, differences are present both in spectra and in the states. This is confirmed by our numerical calculations which also show that the H_p predictions are closer to the full Rabi results.

Our analysis shows that recovering the independent-boson model in the limit $\epsilon \rightarrow 0$ is a valuable test for effective Hamiltonian approaches to the quantum Rabi model.

ACKNOWLEDGMENTS

V.M. acknowledges the financial support from the Romanian Core Program PN19-03 (Contract No. 21 N/08.02.2019).

-
- [1] A. F. Kockum, A. Miranowicz, S. De Liberato, S. Savasta, and F. Nori, *Nat. Rev. Phys.* **1**, 19 (2019).
 - [2] P. Forn-Díaz, L. Lamata, E. Rico, J. Kono, and E. Solano, *Rev. Mod. Phys.* **91**, 025005 (2019).
 - [3] E. T. Jaynes and F. W. Cummings, *Proc. IEEE* **51**, 89 (1963).
 - [4] P. Meystre and M. Sargent, *Elements of Quantum Optics* (Springer, Berlin, 2007).
 - [5] D. F. Walls and Gerald J. Milburn, *Quantum Optics*, 2nd ed. (Springer, Berlin, 2008).
 - [6] D. Braak, *Phys. Rev. Lett.* **107**, 100401 (2011).
 - [7] F. A. Wolf, M. Kollar, and D. Braak, *Phys. Rev. A* **85**, 053817 (2012).
 - [8] Q.-W. Wang and Y.-L. Liu, *J. Phys. A: Math. Theor.* **46**, 435303 (2013).
 - [9] H. Zhong, Q. Xie, M. T. Batchelor, and C. Lee, *J. Phys. A: Math. Theor.* **46**, 415302 (2013).
 - [10] P. Forn-Díaz, J. Lisenfeld, D. Marcos, J. J. García-Ripoll, E. Solano, C. J. P. M. Harmans, and J. E. Mooij, *Phys. Rev. Lett.* **105**, 237001 (2010).
 - [11] L. Garziano, R. Stassi, V. Macrì, A. F. Kockum, S. Savasta, and F. Nori, *Phys. Rev. A* **92**, 063830 (2015).
 - [12] F. Beaudoin, J. M. Gambetta, and A. Blais, *Phys. Rev. A* **84**, 043832 (2011).
 - [13] M. Cirio, S. De Liberato, N. Lambert, and F. Nori, *Phys. Rev. Lett.* **116**, 113601 (2016).
 - [14] I. V. Dinu, V. Moldoveanu, and P. Gartner, *Phys. Rev. B* **97**, 195442 (2018).

- [15] S. De Liberato, D. Gerace, I. Carusotto, and C. Ciuti, *Phys. Rev. A* **80**, 053810 (2009).
- [16] G. D. Mahan, *Many-Particle Physics* (Plenum, New York, 1990).
- [17] B. Krummheuer, V. M. Axt, and T. Kuhn, *Phys. Rev. B* **65**, 195313 (2002).
- [18] A. Mitra, I. Aleiner, and A. J. Millis, *Phys. Rev. B* **69**, 245302 (2004).
- [19] D. Zueco, G. M. Reuther, S. Kohler, and P. Hänggi, *Phys. Rev. A* **80**, 033846 (2009).
- [20] A. Blais, R.-S. Huang, A. Wallraff, S. M. Girvin, and R. J. Schoelkopf, *Phys. Rev. A* **69**, 062320 (2004).
- [21] A. B. Klimov and S. M. Chumakov, *A Group-Theoretical Approach to Quantum Optics: Models of Atom-Field Interactions* (Wiley, New York, 2009).
- [22] D. Z. Rossatto, C. J. Villas-Bôas, M. Sanz, and E. Solano, *Phys. Rev. A* **96**, 013849 (2017).
- [23] J. Hausinger and M. Grifoni, *New J. Phys.* **10**, 115015 (2008).
- [24] E. K. Irish, *Phys. Rev. Lett.* **99**, 173601 (2007).
- [25] L. Yu, S. Zhu, Q. Liang, G. Chen, and S. Jia, *Phys. Rev. A* **86**, 015803 (2012).
- [26] W. Xie *et al.*, *J. Phys. A: Math. Theor.* **53**, 095302 (2020).
- [27] Y.-Y. Zhang, *Phys. Rev. A* **94**, 063824 (2016).
- [28] Y.-Y. Zhang and X.-Y. Chen, *Phys. Rev. A* **96**, 063821 (2017).
- [29] Let us stress that the pure squeezing transform used in Refs. [26,28] fails to cancel the quadratic operators.
- [30] Other technicalities play a role too: the commutator $[\hat{S}, \bar{S}]$ generates only off-diagonal terms, which do not influence the \hat{N}_x expectation value.